Journal of Radiation Research, Vol. 56, No. 5, 2015, pp. 777–783
doi: 10.1093/jrr/rrv039
Advance Access Publication: 9 July 2015

Radiation-induced bystander effect in non-irradiated glioblastoma spheroid cells

Fahime Faqihi[1], Ali Neshastehriz[2]*, Shokouhozaman Soleymanifard[3], Robabeh Shabani[4] and Nazila Eivazzadeh[5]

[1]Radiation Sciences Department, Tehran University of Medical Sciences, Tehran, Iran
[2]Radiation Sciences Department, Faculty of Medical Physics, Iran University of Medical Sciences, Tehran, Iran
[3]Medical Physics Department, Faculty of Medicine, Mashhad University of Medical Sciences, Mashhad, Iran
[4]Cellular and Molecular Research Center, Iran University of Medical Sciences, Tehran, Iran
[5]Radiation Research Center, a.ja University of Medical Sciences, Tehran, Iran
*Corresponding author. Radiation Sciences Department, Faculty of Medical Physics, Iran University of Medical Sciences, Junction of Shahid Hemmat & Shahid, Chamran Expressways, Tehran, IRAN 15785-6171. Tel/Fax: +982188602218; Email: neshastehriz@yahoo.com
Received February 26, 2015; Revised May 2, 2015; Accepted June 7, 2015

ABSTRACT

Radiation-induced bystander effects (RIBEs) are detected in cells that are not irradiated but receive signals from treated cells. The present study explored these bystander effects in a U87MG multicellular tumour spheroid model. A medium transfer technique was employed to induce the bystander effect, and colony formation assay was used to evaluate the effect. Relative changes in expression of *BAX*, *BCL2*, *JNK* and *ERK* genes were analysed using RT-PCR to investigate the RIBE mechanism. A significant decrease in plating efficiency was observed for both bystander and irradiated cells. The survival fraction was calculated for bystander cells to be 69.48% and for irradiated cells to be 34.68%. There was no change in pro-apoptotic *BAX* relative expression, but anti-apoptotic *BCL2* showed downregulation in both irradiated and bystander cells. Pro-apoptotic *JNK* in bystander samples and *ERK* in irradiated samples were upregulated. The clonogenic survival data suggests that there was a classic RIBE in U87MG spheroids exposed to 4 Gy of X-rays, using a medium transfer technique. Changes in the expression of pro- and anti-apoptotic genes indicate involvement of both intrinsic apoptotic and *MAPK* pathways in inducing these effects.

KEYWORDS: radiation-induced bystander effect, U87MG spheroid, apoptosis

INTRODUCTION

Cells traversed by direct irradiation can be affected biologically; non-traversed adjacent cells are also affected by a biological response called the radiation-induced bystander effect (RIBE) [1]. This response is generated through gap junction intercellular communication (GJIC) between the target and adjacent cells by factors (reactive oxygen species (ROS), nitrogen species, or physical factors) secreted into the medium [2–5]. A variety of molecular and cellular endpoints have been documented in bystander cells, including alteration in protein expression [6], sister chromatid exchanges (SCEs) [7], micronuclei [8], apoptosis [9], and a decrease or increase in cell survival [1, 10].

Studies have provided evidence supporting the role of epigenetic regulators such as alteration in gene expression in the production of RIBEs. Evaluation of the changes in gene expression could help define the signalling pathways involved in these effects [2]. The mitogen-activated protein kinase (*MAPK*) pathway plays a vital role in regulating gene expression and in controlling cellular responses such as activation of growth, proliferation, differentiation and apoptosis. Multiple signal transduction pathways activated by ionizing radiation are mediated by the MAPK superfamily, including the extracellular signal–regulated kinase (ERK), c-Jun N-terminal kinase (JNK) [11].

The multiple stresses stimulating *JNK* activity include tumour necrosis factor, interleukin-1, ionizing and ultraviolet radiation, and DNA damage agents. Activation of *JNK* by stress stimuli is associated with apoptotic cell death. By contrast, *ERK* is strongly activated by growth factors and cytokines and plays a major role in regulating cell

growth, survival and differentiation. The expression of these genes is related to tumour cell radio sensitivity [12]. The involvement of calcium and *MAPK* kinase signalling pathways in the production of RIBE has been evaluated, and it has been shown that these effects can induce change in *MAPK* proteins and downstream targets [13].

Furlong *et al*. analysed the transcriptional expression of *JNK* and *ERK* [14]. An unexpected response in which both *ERK* and *JNK* were downregulated was detected in bystander samples. Another study showed that inhibition of *ERK* can increase the number of bystander cells [15]. The intrinsic (mitochondrial) pathway of apoptosis functions in response to radiation following the reception of stress signals activates the pro- and anti-apoptotic *BCL2* family. This interaction destabilizes the mitochondrial membrane and causes release of apoptotic factors [16]. An alteration in the *BCL2* protein level has been detected in bystander human keratinocytes exposed to signalling factors from microbeam-irradiated cells [6].

Differences in the *MAPK* pathway and *BCL2* family genes have been reported in directed and bystander cells for some human cell lines cultured in a monolayer [13, 14, 17], but these are not sufficient for explaining the mechanism of the pathways that affect bystander cells, especially in radioresistant tumours. The present study evaluated the bystander effect in human glioblastoma (U87MG) cells, with a focus on alteration of pro-apoptotic (*BAX* and *JNK*) and anti-apoptotic genes (*BCL2* and *ERK*). A 3D multicellular tumour spheroid model culture was used to mimic the *in vivo* conditions more closely than is possible in 2D culture systems and which is suitable for *in vitro* studies [18]. The medium transfer technique was employed to induce the bystander effect, and colony formation assay was used to evaluate cell death.

MATERIALS AND METHODS

Cell line

The human glioblastoma cell line U87MG (Pasteur Institute; Iran) was routinely cultured in Eagle's minimum essential medium (MEM) enriched with Earle's salts with L-glutamine (PAA; Germany), supplemented with 10% fetal bovine serum (FBS), (PAA; Germany), 500 U/ml penicillin and 200 mg/l streptomycin (Sigma; USA).

Monolayer culture

Cells were cultured in a monolayer at a density of 250 000 cells/ml in T-25 tissue culture flasks. The cultures were maintained at 37°C in a humidified atmosphere of 5% CO_2 to grow at 70–80% confluence to ensure maintenance in the logarithmic phase of growth. Cells were then harvested using a trypsinizing agent of 1 mM EDTA and 0.25% trypsin (w/v) (Sigma; USA) in phosphate buffer saline (PBS). Cell viability >98% was confirmed using trypan blue exclusion criteria.

Spheroid formation

Spheroids were formed using the liquid overlay technique described by Carlsson and Yuhas [17]. The cells were seeded into T-25 tissue culture flasks coated with a layer of 1% agar (Bacto Agar; Difco; USA) and 10 ml of MEM supplemented with 10% FBS. The flasks were incubated at 37°C in a humidified atmosphere of 5% CO_2 and half of the culture medium was replaced with fresh medium twice a week.

Irradiation and medium transfer

Flasks containing spheroids with diameters of ~100 μm were divided into three groups: direct irradiation, bystander, and control. The direct groups were irradiated at room temperature with 6-MV X-rays produced by a linear accelerator (Linac 600, GMV; Varian Medical Systems; USA).

The bystander group received medium from the target group, and the control (sham irradiated and sham bystander) flasks were handled under conditions similar to the target, but without irradiation. Irradiated cell conditioned medium (ICCM) was collected from the target and sham irradiated flasks incubated for 1 h at 37°C after irradiation. The transfer of medium was set up using the transfer technique developed by Mothersill and Seymour [1]. The ICCM pooled for the target and sham irradiated flasks was filtered through 0.22-μm acetate cellulose filters (Orange Scientific; Belgium) and transferred into bystander flasks. Control and target groups were then transferred into the fresh culture medium and incubated at 37°C.

Trypan blue exclusion test of cell viability

The trypan blue test was used to determine the number of viable cells. A suspension of single cells from spheroid cultures was mixed with trypan blue at a ratio of 9 : 1 and the mixture visually examined under a light microscope. A viable cell displays clear cytoplasm and a nonviable cell displays blue cytoplasm. The percentage of cells with clear cytoplasm was reported as a measurement of the viability for each category of cells.

Colony formation assay

To prepare single cells, spheroids were trypsinized with 300 μl of trypsin for 5 min after 24 h of irradiation and media transfer. These single cells were plated for the colony formation test. After 11 d of incubation, cultured cells were washed three times with PBS, fixed with 2% formaldehyde for 10 min, stained with 0.5% crystal violet and left at room temperature for 30 min to dry. The colonies were counted using an inverted microscope (Zeiss, Axiovert 405M; Germany), and those that contained >50 cells were considered to have viable cells.

To investigate the ability of cells to establish colonies, different numbers of single cells (3000, 4000, 5000, 6000) from spheroids seeded onto 60-mm plates with 10 ml of MEM supplemented with 10% FBS were used to obtain an appropriate concentration of cells for evaluation. Plating efficiency was calculated using the following equation:

$$\mathrm{PE}\ (\%) = (\mathrm{numberofcolonies}/\mathrm{numberofseededcells}) \times 100.$$

RNA isolation

For both direct irradiated and bystander flasks, total RNA was isolated at 4 h and 24 h, after irradiation and media transfer. Total RNA was also isolated for control flasks. Spheroids were collected, washed twice with cold PBS, and processed for total RNA isolation using a total RNA extraction kit (Jenabioscience; Germany) according to the manufacturer's instructions. Total RNA was collected from ~4×10^6 cells. RNA optical density was analysed by spectrophotometer.

Table 1. List of forward and reverse oligo sequences of genes used in this study

Gene	Forward oligo sequence	Reverse oligo sequence
BAX	5′ AGGATGCGTCCACCAAGAAG 3′	5′ AGACTGCCGTTGAAGTTGACC 3′
BCL2	5′ TTAGCCCCCGTGACCTCTTA 3′	5′TGTGCTGCTATCCTGCCAAA 3′
ERK	5′ TTAGGGCTGTGAGCTGTTCC 3′	5′ GGTACAGGAGTAGGAGGACT 3′
JNK	5′ TTAAAGCCAGTCAGGCAAGG 3′	5′ GGTTGTGGGCATGTAGTTAC 3′
GAPDH	5′ CGCTCTCTGCTCCTCCTGTT 3′	5′ CCATGGTGTCTGAGCGATGT 3′

Complementary DNA synthesis

DNase treatment of RNA was performed. Up to 1 µg total RNA was converted into cDNA using AccuPower CycleScript RT PreMix (Bioneer; Korea) according to the manufacturer's instructions.

Optimization of primers

BAX, *ERK* and *JNK* primer sequences were obtained from Furlong *et al.* [14], and the *GAPDH* and *BCL2* primer sequences were designed using Primer3 software. *GAPDH* was used as an internal control to normalize target gene expression. Table 1 lists the designated primer sequences. Annealing temperatures for all primers were optimized with thermal gradient PCR.

RT-PCR

SYBR Green technology (AccuPower GreenStar qPCR Master Mix; Bioneer; Korea) was used for all qRT-PCR experiments using a Rotor-Gene (Corbett 6000; Australia). The reaction used 2 µl of cDNA product, 10 µl SYBR Green, 6 µl H_2O and 2 µl of each primer (forward and reverse) for a total volume of 20 µl. The RT-PCR program consisted of a predenaturation step for 10 min at 95°C, denaturation for 15 s at 95°C, annealing for 45 s at 61°C, 60°C and 59°C and extension for 1 min at 72°C. Each sample was set up in triplicate ($n = 3$) and the means calculated.

Data analysis

The cycle threshold (CT) values provided by RT-PCR were used to calculate the relative fold expression according to $2^{-\Delta\Delta CT}$ using normalization for endogenous control *GAPDH* and non-irradiated control samples.

Statistical analysis

The data presented are from three independent experiments. Comparison between groups was performed using one-way ANOVA and the Scheffe *post hoc* test. A value of $P \leq 0.05$ between groups was considered to be significant. The graph was created using Microsoft Excel 2010.

RESULTS

Viability results

The percentage of viability of the cells was assayed using trypan blue dye exclusion as described. The range of viability for the control, radiation and bystander cells was 85.3–92.6%. Only the X-ray group showed a significant decrease in viable cells compared with the control group ($P = 0.04$; Fig. 1).

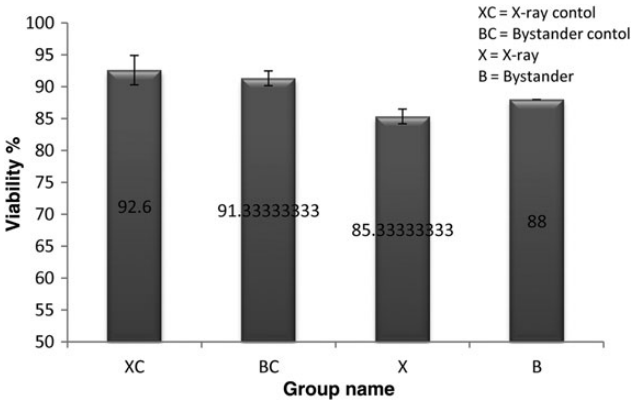

Fig. 1. Viability percent using Trypan Blue dye 24 h after irradiation and medium transfer. Each bar represents the mean ± SD of the results for three independent experiments.

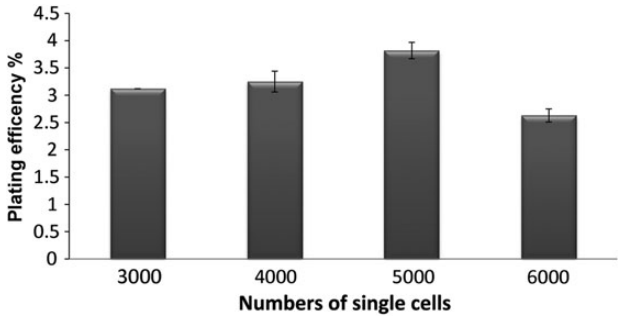

Fig. 2. Plating efficiency using U87MG of various concentrations of cells of spheroids cultured in MEM supplemented with 10% FBS. Each bar represents the mean ± SD of the results for three independent experiments.

Clonogenic survival

The results of colony formation for the various numbers of single cells showed that the optimum cell number for the best plating efficiency in the spheroids was ~5000 (Fig. 2). Table 2 provides the clonogenic survival data for cells treated with radiation or ICCM at 4 Gy. The difference between groups was determined using one-way ANOVA ($F(3,12) = 36.652$, $P = 0.000$).

ICCM was less toxic than direct irradiation, but decreased the survival fraction to 69.48% compared with the control group. It is

evident from the table that the bystander control had the same plating efficiency as the radiation control group.

RT-PCR results

Figures 3–6 compare the relative mean fold changes in gene expression levels for *BAX*, *BCL2*, *JNK* and *ERK* in U87MG spheroids at 4 h and 24 h after 4 Gy irradiation and medium transfer.

BAX and BCL2

The relative expression of *BAX* (Fig. 3) increased in a transient fashion after 4 h in irradiated samples and then returned to the control level at 24 h, but the expression was not significant in the bystander samples ($P > 0.05$). Figure 4 shows that, at first, anti-apoptotic *BCL2* expression increased slightly and then decreased in directly radiated samples at 24 h following irradiation ($P = 0.06$). The bystander cells displayed stable downregulation at 4 h and 24 h ($P < 0.05$).

Downregulation of *BCL2* expression without clear changes in *BAX* expression favoured apoptosis in both direct and bystander samples. The *BAX*/*BCL2* ratio (Fig. 7) shows the degree of vulnerability of cells to apoptosis in both direct and bystander cells.

JNK and ERK

Figure 5 shows the mean fold change in pro-apoptotic *JNK* expression at 4 h and 24 h following irradiation and medium transfer. Significant upregulation was detected in bystander cells at 4 h ($P = 0.04$), but this was not significant for irradiated cells at 4 h ($P = 0.06$). Upregulation had decreased for both samples at 24 h.

The anti-apoptotic *ERK* expression did not display obvious changes in bystander samples at 4 h and 24 h. Expression from these samples increased slightly in comparison with control groups ($P > 0.05$). *ERK* expression was dramatically upregulated at 4 h ($P = 0.000$) in direct cells (Fig. 6).

DISCUSSION

It is crucial to understand the underlying mechanisms for RIBE response for irradiated and non-irradiated tumour cells in order to design a more efficient plan for radiotherapy. The present study indicates that U87MG spheroid signals secreted transmissible factor into the medium generated by 6-MV X-ray radiation that was sufficiently strong to decrease the survival rate for non-irradiated U87MG spheroids over the long-term and to alter apoptosis gene expression as an early response.

A decrease in irradiated cell survival and viability as measured by colony formation assay and trypan blue assay results from the production of free radicals, but this decrement has a different mechanism for bystander cells and is probability initiated by the binding of ligands to cell surface receptors, such as TNF-related apoptosis-inducing ligands [19]. There is evidence that low-LET ionizing radiation can reduce

Table 2. Clonogenic survival data for U87MG spheroid culture exposed to 4 Gy irradiation and ICCM

Group	Mean no. colonies	S	% P	SD	PV[c]	%SF mean[b]	SD
Radiation control	173	19.71	3.46	0.39		-	
Bystander control	165.75	21.82	3.31	0.43	0.952		-
Radiation	60.00	13.83	1.20	0.27	0.000	34.68	8.11
Bystander	115.25	14.17	2.30	0.28	0.001	69.48	8.56

[a]Standard deviation. [b]Plating efficiency mean percent. [c]*P*-value. [d]Survival fraction mean percent. *P*-value ≤ 0.05 was considered significant.

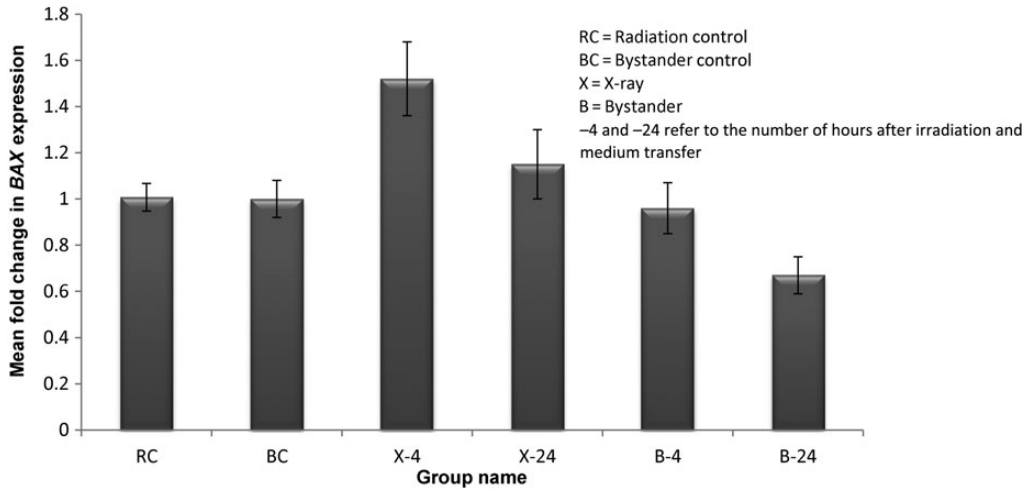

Fig. 3. Relative fold-changes in gene expression levels of *BAX* in U87MG spheroid following 4-h and 24-h exposure to 4 Gy direct and bystander X-ray irradiation. Each bar represents the mean ± SD of the results of three independent experiments. Asterisk represents significant changes.

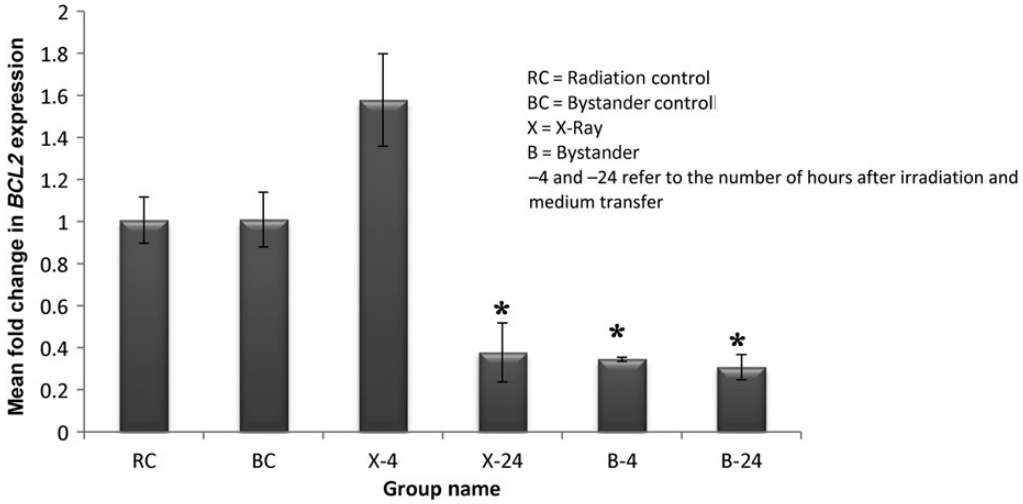

Fig. 4. Relative fold-changes in gene expression levels of *BCL2* in U87MG spheroid following 4-h and 24-h exposure to 4 Gy direct and bystander X-ray irradiation. Each bar represents the mean ± SD of the results of three independent experiments. Asterisk represents significant changes.

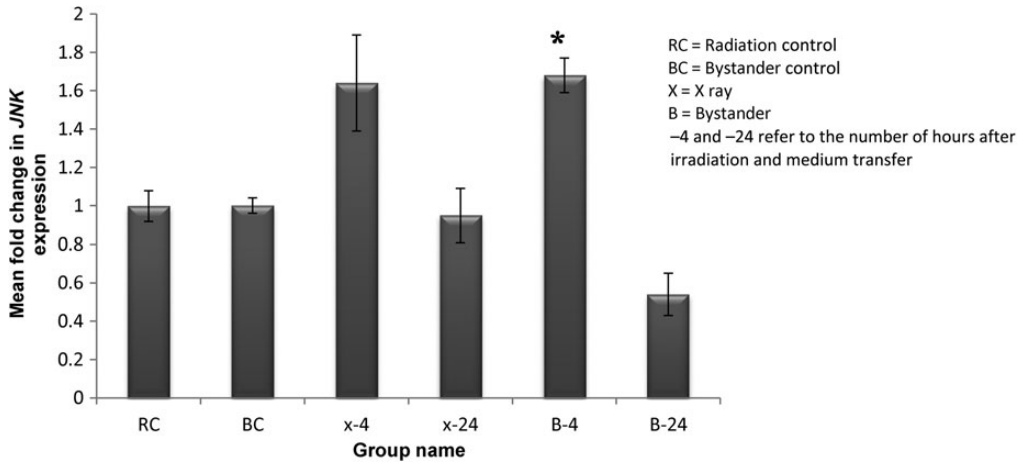

Fig. 5. Relative fold-changes in gene expression levels of *JNK* in U87MG spheroid following 4-h and 24-h exposure to 4 Gy direct and bystander X-ray irradiation. Each bar represents the mean ± SD of the results of three independent experiments. Asterisk represents significant changes.

the number of bystander cells in several normal and tumour cell lines, but there has been no evidence for radiation-induced cell death in bystander U87MG cells to date.

Boyd tested a dosage range of 0–9 Gy of external beam radiation to donor cells and found it caused 30–40% clonogenic cell kill in bystander cultures in the UVW/NAT glioma cell line [20]. Gow *et al.* reported bystander cell death in T98G glioma cells after exposure to ICCM by high-energy 20-MeV electrons at a dose rate of 10 Gy min^{-1}, but their initial experiments produced no significant differences in bystander cell death from control levels for ^{60}Co-ɣ rays and 20-MeV electrons at 1.7 Gy min^{-1}. The author suggested a threshold of radiation stress was required to induce bystander cell death [21].

Ivanov and Hei did not detect non-targeted effects for irradiated U87MG on non-irradiated glioblastoma cells for cell death [22]. The major difference between Ivanov *et al.*'s study and the present study is the type of cell culture model (monolayer versus spheroid). MCTS is generally considered to be a better model than 2D culture for predicting an *in vivo* response to treatment. Increased radioresistance of a spheroid culture in comparison with a monolayer culture has been reported [23], but there has been no evidence reported for bystander effects. A different mechanism exists for bystander effects in comparison with direct radiation effects and the importance of GJIC in bystander response. Further investigation of spheroid culture and the medium surrounding irradiated cells would be helpful.

The present study examined the relative expression of four apoptosis genes followed by either direct or bystander exposure to 4 Gy X-ray radiation. The *ERK* pathway is a *MAPK* signal transduction pathway that conveys signals from the cell surface to intracellular targets [12]. The activation of *ERK* protein depends on cell type [17]

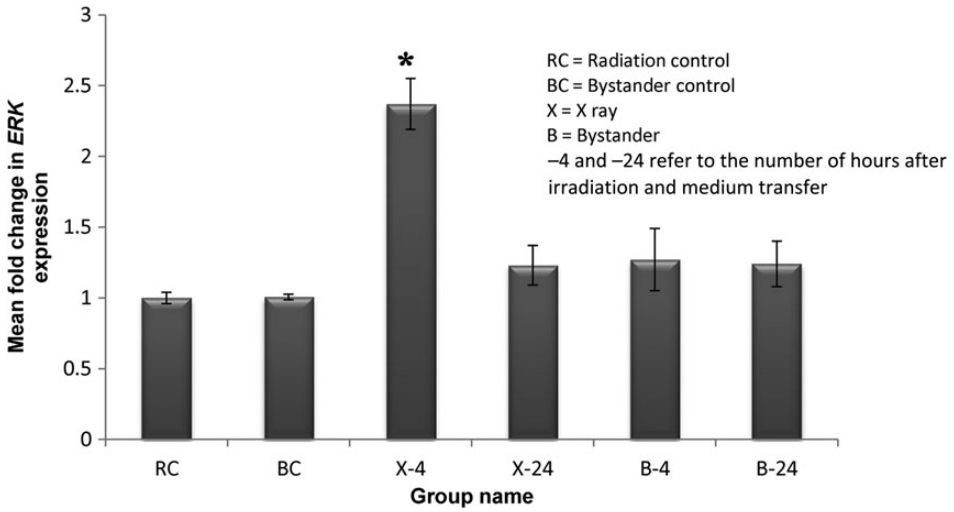

Fig. 6. Relative fold-changes in gene expression levels of *ERK* in U87MG spheroid following 4-h and 24-h exposure to 4 Gy direct and bystander X-ray irradiation. Each bar represents the mean ± SD of the results of three independent experiments. Asterisk represents significant changes.

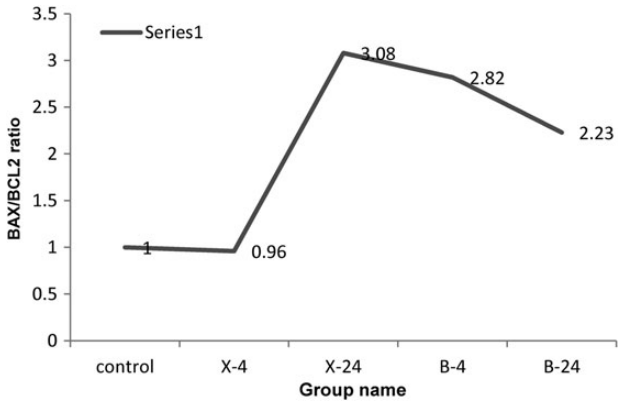

Fig. 7. BAX/BCL2 relative fold expression ratio in U87MG spheroid following 4-h and 24-h exposures to 4 Gy direct and bystander X-ray irradiation Each bar represents the mean ± SD of the results of three independent experiments.

and has a transient nature [24]. The results indicate that relative expression varied between direct and bystander cells.

Transient upregulation of the *ERK* gene in direct samples emphasizes the radioresistance of this cell line. Studies carried out on glioma cells provide evidence for the role of this gene in modulating radiation-induced double-strand breakage and cell survival [15, 25]. The expression of this gene in response to bystander factors did not change in bystander samples at 4 h and 24 h. A previous study observed downregulation in the expression of *ERK* in bystander cells of irradiated normal human lymphoblastoid cells [17]. These contradictory results are due to the different cell lines used.

The *JNK* pathway is often called the stress-activated protein kinase pathway. Ionizing radiation activates their genes under a known mechanism [26]. The *JNK* genes are also activated by ROS, which have been found to be important signalling molecules involved in the production of bystander signals in glioma cells [27]. The *JNK* pathway activates caspases and regulates proteins implicated in apoptosis regulation, including *P53*, *BCL2* and *BAX*. This can be attributed to *JNK*-mediated *BAX*, *BAK* activation and *BCL2* downregulation in response to ionizing radiation.

The present study expected upregulation of *JNK* in bystander samples and a rising trend in direct samples at 4 h (as an early response) that would affect regulation of *BCL2* for both direct and bystander samples. The *JNK* was downregulated in bystander HaCaT cells, which could be the result of administration of such a low dose that the signal from the direct cells was not strong enough to induce the pro-apoptotic function of *JNK* in bystander cells [14]. The high dose used in the present investigation activated *JNK* expression. Higher activation in *JNK* suggests its distinct function in bystander cell death.

The pro-apoptotic *BAX* protein expression level is controlled by transcription factor *P53*. Ivanov *et al.* demonstrated suppression of *P53–BAX*-dependent apoptotic signalling in U87MG after irradiation [22]; thus, the lack of change in *BAX* expression in both direct and bystander cells can be justified. *BCL2* gene expression in bystander cells showed significant downregulation at 4 h and 24 h ($P < 0.05$), but cells directly exposed showed a decreasing trend without significant change. As explained, early *JNK* upregulation could lead to downregulation of *BCL2* in bystander and direct groups.

The *BAX/BCL2* ratio is most strongly related to apoptotic progression, which makes investigation of mitochondrial death genes more useful. An increasing *BAX/BCL2* ratio in bystander spheroids at 4 h and 24 h following medium transfer indicates that apoptosis has been initiated. These data show the ability of irradiated U87MG spheroids to produce bystander signals that lead to a response by non-irradiated U87MG spheroids. From the downregulation of *BCL2* and upregulation of *JNK* in bystander groups versus upregulation of *ERK* in directly irradiated samples, it can be concluded that bystander cells have greater affinity for apoptosis. This should be confirmed by measuring the levels of apoptosis.

ACKNOWLEDGEMENTS

We are grateful to Dr Ali Samadi Kuochaksaraee for his helpful advice and contribution during this research.

REFERENCES

1. Mothersill C, Seymour C. Medium from irradiated human epithelial cells but not human fibroblasts reduces the clonogenic survival of unirradiated cells. *Int J Radiat Biol* 1997;71:421–7.
2. Asur RS, Sharma S, Chang C-W, et al. Spatially fractionated radiation induces cytotoxicity and changes in gene expression in bystander and radiation adjacent murine carcinoma cells. *Radiat Res* 2012;177:751–65.
3. Mothersill C, Smith RW, Fazzari J, et al. Evidence for a physical component to the radiation-induced bystander effect? *Int J Radiat Biol* 2012;88:583–91.
4. Shao C, Folkard M, Michael BD, et al. Bystander signaling between glioma cells and fibroblasts targeted with counted particles. *Int J Cancer* 2005;116:45–51.
5. Shao C, Folkard M, Prise K. Role of TGF-β1 and nitric oxide in the bystander response of irradiated glioma cells. *Oncogene* 2007;27:434–40.
6. Lyng FM, Maguire P, Kilmurray N, et al. Apoptosis is initiated in human keratinocytes exposed to signalling factors from microbeam irradiated cells. *Int J Radiat Biol* 2006;82:393–9.
7. Nagasawa H, Little JB. Induction of sister chromatid exchanges by extremely low doses of α-particles. *Cancer Res* 1992;52:6394–6.
8. Soleymanifard S, Bahreyni MTT. Comparing the level of bystander effect in a couple of tumor and normal cell lines. *J Med Phys* 2012;37:102–6.
9. Lyng F, Seymour C, Mothersill C. Production of a signal by irradiated cells which leads to a response in unirradiated cells characteristic of initiation of apoptosis. *Br J Cancer* 2000;83:1223–30.
10. Mackonis EC, Suchowerska N, Zhang M, et al. Cellular response to modulated radiation fields. *Phys Med Biol* 2007;52:5469–82.
11. Dent P, Yacoub A, Fisher PB, et al. MAPK pathways in radiation responses. *Oncogene* 2003;22:5885–96.
12. Munshi A, Ramesh R. Mitogen-activated protein kinases and their role in radiation response. *Genes Cancer* 2013;4:401–8.
13. Lyng FM, Maguire P, McClean B, et al. The involvement of calcium and MAP kinase signaling pathways in the production of radiation-induced bystander effects. *Radiat Res* 2006;165:400–9.
14. Furlong H, Mothersill C, Lyng FM, et al. Apoptosis is signalled early by low doses of ionising radiation in a radiation-induced bystander effect. *Mutat Res* 2013;741:35–43.
15. Zhou H, Suzuki M, Geard CR, et al. Effects of irradiated medium with or without cells on bystander cell responses. *Mutat Res* 2002;499:135–41.
16. Elmore S. Apoptosis: a review of programmed cell death. *Toxicol Pathol* 2007;35:495–516.
17. Asur R, Balasubramaniam M, Marples B, et al. Bystander effects induced by chemicals and ionizing radiation: evaluation of changes in gene expression of downstream MAPK targets. *Mutagenesis* 2010:25:271–9.
18. Boyd M, Sorensen A, McCluskey AG, et al. Radiation quality-dependent bystander effects elicited by targeted radionuclides. *J Pharm Pharmacol* 2008;60:951–8.
19. Gómez-Millán J, Katz ISS, de Araujo Farias V, et al. The importance of bystander effects in radiation therapy in melanoma skin-cancer cells and umbilical-cord stromal stem cells. *Radiother Oncol* 2012;102:450–8.
20. Boyd M, Ross SC, Dorrens J, et al. Radiation-induced biologic bystander effect elicited *in vitro* by targeted radiopharmaceuticals labeled with α-, β-, and Auger electron–emitting radionuclides. *J Nucl Med* 2006;47:1007–15.
21. Gow M, Seymour C, Ryan L, et al. Induction of bystander response in human glioma cells using high-energy electrons: a role for TGF-β1. *Radiat Res* 2010;173:769–78.
22. Ivanov VN, Hei TK. Radiation-induced glioblastoma signaling cascade regulates viability, apoptosis and differentiation of neural stem cells (NSC). *Apoptosis* 2014;19:1736–54.
23. Santini MT, Rainaldi G. Three-dimensional spheroid model in tumor biology. *Pathobiology* 1999;67:148–57.
24. Cagnol S, Chambard JC. ERK and cell death: mechanisms of ERK-induced cell death—apoptosis, autophagy and senescence. *FEBS J* 2010;277:2–21.
25. Golding SE, Morgan RN, Adams BR, et al. Pro-survival AKT and ERK signaling from EGFR and mutant EGFRvIII enhances DNA double-strand break repair in human glioma cells. *Cancer Biol Ther* 2009;8:730–8.
26. Chen Y-R, Meyer CF, Tan T-H. Persistent activation of c-Jun N-terminal kinase 1 (JNK1) in γ radiation-induced apoptosis. *J Biol Chem* 1996;271:631–4.
27. Shao C, Lyng FM, Folkard M, et al. Calcium fluxes modulate the radiation-induced bystander responses in targeted glioma and fibroblast cells. *Radiat Res* 2006;166:479–87.